Eötvös Loránd Univertsity

Faculty of Natural Sciences

Center of Environmental Studies

INVESTIGATION OF THE INTERACTION BETWEEN GROUNDWATER AND SURFACE WATER AT DISCHARGE AREA IN HUNGARY

THESIS

Made by:

AMANDA LAFETÁ OLIVEIRA

Environmental Sciences MSc

Supervisor:

Dr. Ákos Horváth

Budapest

2020

Contents

List of figures

List of tables

ABSTRACT

^{222}Rn has been used to detect groundwater exfiltration, study the changes of its content in waters after seismic activities, in case of water flow in underwater caves and for developing a better understanding of subsurface and surface water interactions in a coastal aquifer. Radon can help to evaluate the recharge dynamics of a karst aquifer and provided information on a time scale of infiltration into the aquifer. In fact, radon has been used to study water dynamics, its processes, interactions, and connections in surface and subsurface systems. (Ferreira, et al. 2018)

This present study evaluated measurement techniques that are used nowadays to analyze the relationship between groundwater and surface water in two different regions in Hungary.

Two sampling places were selected to acquire the samples: Danube river and Eva Spring. Samples were taken in a 10 ml syringe and mixed with a scintillation liquid in an individual vial. The vials were taken into the lab where the measurements took place. The liquid scintillator TriCarb 1000 was used to read the radon counts in each sample. After the measurement, calculations were done to acquire the correct radon concentration of the 3 samples from the Danube river and 7 from the Eva spring.

It was possible to characterize the samples as significant radon concentration (I) and close to background radon concentration (II) due to its measurements. Only two samples could be described as significant radon concentration (A.ES1 and A.ES5). Both could be found in areas where the majority of the water income came from the groundwater.

1. INTRODUCTION (LITERATURE REVIEW)

^{222}Rn has been used to detect groundwater exfiltration, study the changes of its content in waters after seismic activities, in case of water flow in underwater caves and for developing a better understanding of subsurface and surface water interactions in a coastal aquifer. Radon can help to evaluate the recharge dynamics of a karst aquifer and provided information on a time scale of infiltration into the aquifer. In fact, radon has been used to study water dynamics, its processes, interactions and connections in surface and subsurface systems. (Ferreira, et al. 2018)

The interaction between groundwater and lakes has been studied since the 1960s. the main concerns are related to eutrophication and acid rain. The relationship of groundwater to wetlands and to coastal areas has increased in the past 20 years as these ecosystems are lost to development. Groundwater (GW) and surface water (SW) are not isolated components of the hydrologic system, but instead interact in a variety of physiographic and climatic landscapes. Development and contaminations that reaches one affects the other. Understanding the interactions and basic principles of hydrology is necessary to a good management of water resources. It is part of the system GW–SW studies of headwater streams, lakes, wetlands, and estuaries. Surface and subsurface waters can interact when there is a lateral flow from the saturated soil by infiltration or exfiltration. In karstic areas or fractured terrains, the interaction can happen through flow in fracture channels. (Sophocleous, 2002)

Water that enters a surface-water body promptly, in response to such individual water input events as rain or snowmelt, is known as event flow, direct flow, storm flow, or quick flow. This water is distinguished from baseflow, or water that enters a stream from persistent, slowly varying sources and maintains stream flow between water-input events. Although some baseflow is derived from drainage of lakes or wetlands, or even from the slow drainage of relatively thin soils on upland hill slopes, most baseflow is supplied from groundwater flow. Subsurface flow can also enter streams quickly enough to contribute to the event response. Such flow is called subsurface storm flow or interflow. (Sophocleous, 2002)

Much of the research performed over the past decade or so has relied on the use of natural radiogenic isotopes of radon and radium to assess the levels of groundwater discharge. Radon (^{222}Rn; $T_{1/2}$ = 3.84 days) works well for this purpose because groundwater typically has activity levels 2–3 orders of magnitude above those of most surface waters. In addition to coastal zone

studies, radon has also been applied to assess groundwater discharge into lakes, streams and rivers, drainage canals and other areas of groundwater–surface water interactions. Technological advances have made measurement of both radon and radium radionuclides much more efficient and convenient. (Chanyotha, et al., 2014)

1.1. Radium

Radioactive substances, like radium, constitute a continuous source of energy. This energy is manifested as radiation. (Curie, 1905)

Radium is a chemical element from the alkaline earth metal family discovered by Marie Curie and Pierre Curie in 1898. It emits γ radiation and α-particles and suffers $3.7x10^{10}$ disintegrations per second. Radium has 25 isotopes and one of them, ^{226}Ra has the longest half-life? 1600 years. It can be absorbed by clay and organic materials with great tenacity being found on roots, grains, hay and some vegetables that were cultivated on soil contaminated by uranium. (Mafra, 2011)

1.2. Radon properties

A tracer that has been used prominently in hydrogeology is ^{222}Rn. It is produced by the alpha decay of the ^{226}Ra in the ^{238}U series. It is a chemically inert element, which does not cause undesirable biogeochemical reactions and does not change its physical characteristics.

Radon is enriched in groundwater when compared to surface waters. This characteristic exists because groundwater is in direct contact with mineral grains containing radium which produces radon gas by decay. On the other hand, surface water is subject to turbulence promoted by environmental factors, which allows the evaporation of radon. The enrichment of radon in groundwater will depend on the contents of its progenitor, radium, which is widely distributed in minerals in aquifer rocks. Radium is present in high concentrations (ppm) in granitic rocks and is less abundant in many metamorphic and sedimentary rocks. Radon has a medium solubility in cold water which decreases when the temperature becomes higher, and this solubility helps it to escape from the rock structure after the decay of radio atoms, through fissures or nanopores, to the surface waters. (Ferreira, et al., 2018)

Another isotope of radon is the thoron, ^{220}Rn ($T_{1/2}$ = 56 s). It has also been applied for discharge identification purposes. It can identify old waters. The accumulation of scale on the inside of pipelines served to concentrate radium over many years. This produced an in situ "radon-generator" that led to higher activities of radon (both ^{220}Rn and ^{222}Rn) coming out of the pipes than was present in the source water. While there were relatively high activities of thoron detected in these old pipelines, its use for groundwater discharge studies has been limited because of the difficultly in measuring a nuclide with such a short half-life. However, the advantage of searching for thoron is that it shows that there is a nearby source. Because of its rapid decay, ^{220}Rn unsupported by its parent ^{224}Ra, would essentially disappear in about 5 min (5 times the half-life). Thus, thoron is potentially an excellent estimating tool. In the case of measurements in natural waters, sources of thoron (as radon) would likely indicate groundwater seeps although other possibilities exist such as accumulations of thorium-enriched minerals (Chanyotha, et al., 2014)

1.3. Partial pressure of radon in water

The partial pressure of a gas in water is a measure of thermodynamic activity of the gas' molecules. Gases dissolve, diffuse and react according to their partial pressures, and not according to their concentrations in gas mixture or liquids. This general property of gases is also true in chemical reactions of gases in biology and physical chemistry and follows the Henry's law (Lide, 1995)

Henry's law:

$$c_w\left[\frac{mol}{m^3}\right] = \kappa\left[\frac{mol}{m^3 Pa}\right] p_{air} \qquad \text{Eq.1}$$

p is the radon's partial pressure in the air phase, c_w is the radon concentration in water, κ is the solubility constant. The solubility constant depends on the temperature and is considered as follow (Table 1)

Table 1 Solubility of radon in water. Source (Lide, 1995)

Radon (222Rn)	Temperature (K)	Solubility
Temperature range 273.15 – 373.15	288.15	2.299×10^{-4}
	293.15	1.945×10^{-4}
	298.15	1.671×10^{-4}
	303.15	1.457×10^{-4}
	308.15	1.288×10^{-4}

We use generally a_w and a_{air} concentrations for water and air respectively. For radon, $a_w = A_w/V_w$, and $a_{air} = A_{air}/V_{air}$.

$$p_{air} = \frac{n_{air}RT}{V_{air}} = \frac{\lambda N_{air}RT}{\lambda N_A V_{air}} = \frac{A_{air}RT}{\lambda N_A V_{air}} = \frac{RT}{\lambda N_A} a_{air}$$

$$c_w = \frac{n_w}{V_w} = \frac{\lambda N_w}{\lambda N_A V_w} = \frac{1}{\lambda N_A} a_w$$

With these:

$$c_w = \frac{1}{\lambda N_A} a_w = \kappa p_{air} = \kappa \frac{RT}{\lambda N_A} a_{air}$$

Therefore, the ratio of the radon concentration in equilibrium is about 4.5, as shown below

$$a_w = \kappa RT a_{air}$$

$$\frac{a_{air}}{a_w} = \alpha(T) = \frac{1}{\kappa(T)RT} \qquad \alpha(T = 293K) = \frac{1}{9.1 \cdot 10^{-5} \frac{mol}{m^3 \cdot Pa} \cdot 8.31 \frac{J}{mol \cdot K} \cdot 293K} = 4.5$$

In a bubbling radon measurement using e.g. RAD7 detector:

$$c_0 V_w + c_B V_a = A_{tot} = c_e V_w + c_m V_a$$

$$c_0 = \frac{\frac{c_m}{\alpha} V_w + c_m V_a - c_B V_a}{V_w} = c_m \left(\frac{1}{\alpha} + \frac{V_a}{V_w} \right) - c_B \frac{V_a}{V_w}$$

1.4. Radioactivity (origin)

The stable isotopes of chemical elements were born in a supernova explosion in the Milky Way galaxy billions of years ago or merge of neutron stars. Natural radioactivity originates from extraterrestrial sources as well as from radioactive elements in the earth's crust. About 340 nuclides have been found in nature, of which about 70 are radioactive and are found mainly among the heavy elements. All elements having an atomic number heavier than 83 are radioactive. (Rahman, et al., 2008)

1.5. Natural series

There are four natural radioactive series or families, Thorium (^{232}Th, $T_{1/2}$ =14.0 billion years), Uranium (^{235}U, $T_{1/2}$ = 4.47 billion years), Actinium (^{238}U, $T_{1/2}$ = 0.7 billion years) and Neptunium (^{237}Np, $T_{1/2}$ = 2 million years) that originate other elements with radioactive characteristics. The natural series occur when an instable element emits a particle (alpha or beta) to become stable after several decays. This emission is associated with the decay of the element that depends on the half-life of each nuclide. After a sequence of decays, the nuclide is now stable, and it is an isotope of lead (^{206}Pb, ^{207}Pb and ^{208}Pb). The decaying series can be seen in the Figure 1 **below**. (Mafra, 2011)

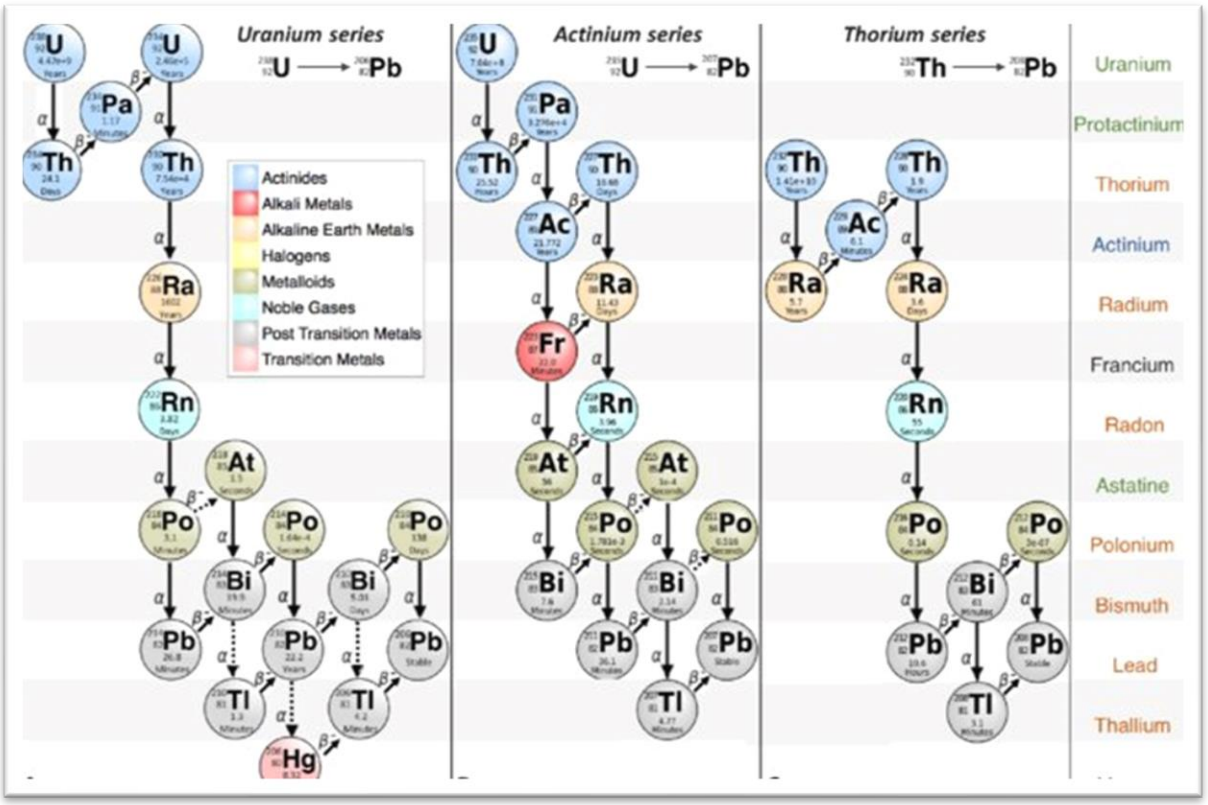

Figure 1 Representative decaying series of the existing radionuclides

1.6. Types of decay

Alpha decay (α): represents the disintegration of a parent nucleus to a daughter through the emission of the nucleus of a helium atom. It consists of two protons and two neutrons bound together into a particle. Because of its very large mass, it heavily ionizes materials and has a very short range.

Beta decay (β): represents the disintegration of a parent nucleus to a daughter though the emission of the beta particle. It consists of a high-energy, high-speed electrons or positrons emitted by certain types of radioactive nuclei. The β particles have greater range of penetration than α particles, but less than gamma rays.

The decaying process can occur randomly when the isotopes are instable and there is not possible to predict the exact time that it happens. However, the average can be calculated like in the **equation 1** below. So, if a sample has N radioactive nuclei its decaying rate is proportional in a time interval (t) to a constant (λ). (Mafra, 2011)

$$-\frac{dN}{dt} = \lambda N \qquad \text{Eq.2}$$

1.7. Activity (A)

Activity is a quantity related to radioactivity for which the SI unit is the becquerel (Bq), equal to one reciprocal second. The becquerel is defined as the number of radioactive disintegrations per second that occur in a particular radionuclide. The older, non-SI unit of activity is the Curie (Ci) which is 3.7×10^{10} decays per second.

Since the probability of radioactive decay for a given radionuclide is a fixed physical quantity (with some slight exceptions, see changing decay rates), the number of decays that occur in a given time of a specific number of atoms of that radionuclide is also a fixed physical quantity (if there are large enough numbers of atoms to neglect statistical fluctuations).

Therefore, the radioactive activity can be expressed integrating the equation above.

$$A = \lambda . N_0 . e^{-\lambda t} \qquad \text{Eq.3}$$

$$A = A_0 . e^{-\lambda t} \qquad \text{Eq.4}$$

1.8. Half life

The half-life ($T_{1/2}$) is the time that radioactive nuclei (N) and the radioactive activity (A) have its value decreased by half of the initial value. It is a statistical property used to estimate the large number of atoms that are involved on the radioactive decay.

It is possible to make a connection between the half-life and the decaying constant (λ) when considering the half-life, the time in the equation 3

1.9. Analytical methods

1.9.1. Rad7

Rad7 (Figure 2) is a highly versatile device that can form the basis of a comprehensive radon measurement system. It has an air pump and a solid-state alpha detector which consists of a semiconductor material. Silicon is usually used as the semiconductor material that converts the alpha radiation to an electrical signal (Salih, et al., 2016)

The main components of the detector are the air filter (1), the air pump (2) and the detector chamber (3). The first block the radon daughters out from the detector chamber, the second makes the air circulate across the pipe system and the third is where an electric field pushes the positive ions down onto the semiconductor detector in the chamber. Inside the chamber, the radon atoms will produce ^{218}Po that is a positively charged ion. In the chamber the electric field will force these ions to be collected on the bottom of the chamber where it accumulates. The energy resolution for this technique is an advantage since the alpha particles will stop in the thin layer of the detector but the beta particles will penetrate through and will not deposit their energy in the detector. (Csanád, et al., 2012)

Figure 2 Rad7 - water measurement setup

1.9.2. Liquid Scintillation Spectroscopy (LSC) – TriCarb 1000

Liquid scintillation counting is the detection of an ionizing radiation through the scintillation light produced in certain solutions. The number of photons emitted during the process is dependent on the type of primary ionizing particle and its energy. Liquid scintillation has the advantage over solid scintillators of mixing the sample within the sensitive medium. Therefore, this technique enables the detection of low energy radiations by avoiding self-absorption in the sample or interface issues. On the other hand, factors like the amount of scintillator solute present in the solution, the presence os impurities in the sample impact the detection efficiency of the process. (Chapon, et al., 2016)

The detector consists in two parts: the scintillator material and the photomultiplier tube (PMT). In the scintillator material, the molecules can emit visible light after excitation or UV photons after one radioactive decay. The PMT (Figure 3) converts this light into electric pulse and the system will analyze the pulse and count them (Csanád, et al., 2012)

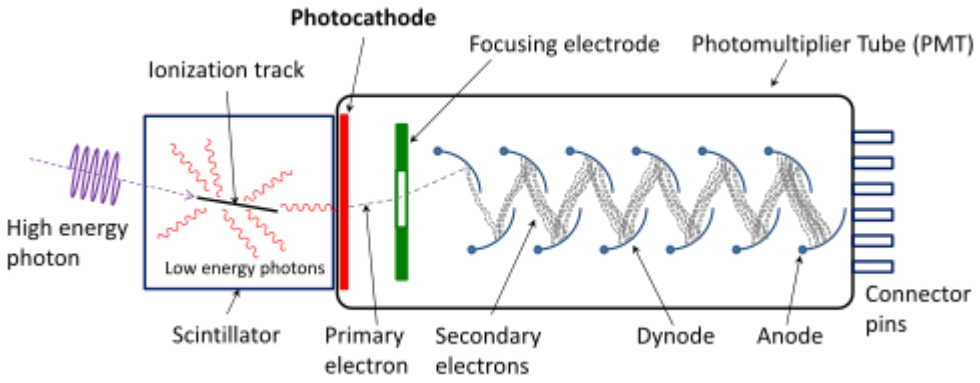

Figure 3 Photomultiplier tube

Beside the sample measurement, the LSC can also detect the background noise that can be mistakenly attributed to the radioactivity emanating from the measured sample. The background can have many sources such as cosmic radiation, ambient background radiation, the material shielding the photomultipliers (PMTs), the glass of the vial or the composition of the cocktail. The phenomenon of chemiluminescence in the emission of photons produced during chemical

processes in the cocktail and the phenomenon of photoluminescence due to excitation of the cocktail with UV light. (Chapon, et al., 2016)

Figure 4 Liquid scintillator TriCarb 1000 TR

1.9.3. Radium delayed coincidence counter (RaDeCC)

Garcia-Solsona, et al. 2008 describes the detection technique for the measurement of ^{223}Ra ($T_{1/2}$=11.43 days) and ^{224}Ra ($T_{1/2}$=3.66 days). The radioisotopes in the water sample will be attached to Mn-fibers and they are counted on a Radium Delayed Coincidence Counter (RaDeCC). This system was pioneered by Giffin et al. (1963) and adapted for radium measurements by Moore and Arnold (1996). The partially dried Mn-fibers are placed in a closed helium-circulation loop. The gas is pumped through a flow meter to the sample chamber containing the Mn-fibers where the flux of helium strips the short-lived radium (^{223}Ra and ^{224}Ra) daughters ^{219}Rn and ^{220}Rn, respectively from the fiber and carries them to a ZnS coated 1.1 L scintillation cell (Lucas cell). By regulating the gas flow-rate at 6 L min^{-1} (i.e. a helium flow of 3.4 L min−1; Moore, 2008-this issue) they achieve an optimal residence time of the gas in the counting system of 24.6 s (6 half-lives of ^{219}Rn). Thereby, the ^{220}Rn–^{216}Po and ^{219}Rn–^{215}Po pairs mostly decay in the cell and they can be used to uniquely identify the radon isotope. The alpha particles are registered using a photomultiplier tube (PMT) attached to the scintillation cell and the delayed coincidence circuit sorts the signals generated by the decay of each of these radon isotopes to a short-lived polonium

isotope: the ^{219}Rn isotope decays to ^{215}Po ($T_{1/2}$=1.8 ms) and ^{220}Rn decays to ^{216}Po ($T_{1/2}$=150 ms). The timeframe of each decay represents the 219 window and the 220 window

Any alpha particle detected in the scintillation cell produces a signal which is routed to a total count register and to the 219 and 220 circuits. The ^{219}Rn and ^{220}Rn decays will be followed by Po alpha-decays shortly after the radon decay, therefore these isotopes will produce coincidences, on a timescale of the half live of their daughters, which are less than 1 sec. The total channel records every decay event (total counts, cpm total). In the two other circuits, the 219 and 220 channels, the signal is delayed to allow the circuit to stabilize or filter any undesirable event (such as an electronic spike in the circuit). The signal then opens an electronic gate in each channel that will remain open for 5.6 ms (219 circuit) and 600 ms (220 channel). Any second event occurred in these time intervals will be counted in the respective circuit (219 counts and cpm 219; 220 counts and cpm 220). The interferences between channels are adequately subtracted. Also, random counts, i.e. "chance" events due to background counts and the decay of ^{222}Rn, are subtracted to obtain the correct events in each channel. Once the corrected 219 and 220 counts are calculated, the activities of ^{223}Ra and ^{224}Ra on the Mn-fiber can be determined.

According to Geibert, et al. (2013), the RaDeCC system records the decay events in three channels. These channels are based on the time difference between two signals due to the half-lives decay product in the relative decay chain. The first channel counts the events from the decay chain of ^{223}Ra, the second counts the events from the decay chain of ^{224}Ra and the third channel counts the total events. Therefore, the signal on the first and second channels are accompanied by a signal on the third channel (Total channel), but also a signal from the ingrowth of ^{222}Rn from the ^{226}Ra decay products. The measurement could demand a lot of time if the equilibrium state is desired. (Geibert, et al., 2013)

1.10. Area of Study

1.10.1. Danube River side

The Danube river is the second largest river in Europe with 2888 km of extension crossing the continent from west to east with its delta at the Dark Sea (Romania). The river basin is a vast region, whose settlement began in very remote times. Its great strategic importance is due to the fact that, in forming most of Central Europe, it has always served as a natural route between Northern Europe, Eastern Europe, Western Europe and Mediterranean or Southern Europe. But, because it is in the center, the Danube basin has become a land of invasions, of coexistence (not always peaceful) of numerous culturally and ethnically different human groups, of overlapping or juxtaposition of different political systems, and of development different ways of life.

Although the Danube served as a natural boundary to define the territory of the Roman Empire during antiquity, it could not avoid the interpenetration of distinct groups on both sides of the river: Romans of Roman origin to the north, Romanians and Slavs to the south

1.10.2. Velencei Hills and Lake Velencei

The Velencei Hills represent one of the two superficial granitic bodies of Hungary (Mórágy Block is the other one in the southern part of Hungary). Both were developed during the Orogeny. Granite occurs in many places in the basin ranges; however, it can only be studied in boreholes or sidewalls. Therefore the Velencei Hills are so important with respect to the study of granites. (Gyalog & Horvath, 2004)

Based on the relief the hills can be divided into two major parts: the West and the East Velence areas. Both can be divided into two other parts. In the West Velence area can be found the Székesfehérvar and West Velence units, where in the East Velence can be found the East Velence units and the Nadap-Pázmánd hill chain.

2. OBJECTIVES

Main objectives:

- Verify the interaction between ground water and surface water in distinct regions in Hungary.

Secondary objectives:

- Choose a valid method to analyze the samples

3. METHODOLOGY

In order to do the measurements, two different places were selected to analyze the groundwater inflow and how much radon can be found in surface water.

This analysis was used to measure the radon atoms that diffuse from the water sample into the cocktail phase of the vial. Each measurement took 15 minutes and gave the values of detection intensity of the samples in counts per minute (CPM) and the uncertainty (%).

3.1. Water sampling

3.1.1. Danube testing samples

On December 13, 2019, test samples were taken from the Danube river between the Erzsébet bridge and the Szabadság bridge to verify the radon concentration at that area (Figure 5).

Figure 5 Sampling location at the Danube River

The water sampling was done using a device developed by the team that consists in a 12 mL syringe attached on an aluminum rod with fishing line to operate it (Figure 6). The water sampled was inserted into a vial that was previously prepared with 10 mL of the cocktail OptiFluor-O and sealed with wax (Figure 7).

Figure 6 Sampling device

Figure 7 Vials with sampled water and OptiFluor-O cocktail

During the sampling requirement the time and coordinates were registered for each sample, as shown on the table below:

Table 2 Danube sample information (December 13th, 2019)

Sample	Coordinates	Time
T1A	47º29'11.38" N 19º3'5.86" E	15:35
T2A	47º29'12.39" N 19º3'4.85" E	15:45
T3A	47º29'13.61" N 19º3'3.51" E	15:53

The samples were analyzed using the TriCarb for 15 minutes and for 3 hours. The background measurement of the equipment was done during a parallel study (by Helen Barbosa) and the results are shown on the *Table 3***Error! Reference source not found.** below:

Table 3 Background measurement for Radon (Source: Helen Barbosa)

Start	Vial	Cocktail	Average (CPM)	Variance
September 13	IF DW	Instafluor	10.18	0.45
September 15	OO DW	OptiFuor-O	11.29	0.47
September 20	2003 DW	OptiFluor-O	10.05	0.43

3.1.2. Eva spring sampling – Sukoró, Hungary

On 12 of April 2020, 7 samples were collected from Eva Spring in the city of Sukoró, Hungary. The city is at the north side of the Lake Velencei and it has 1300 inhabitants nowadays. The distance between the spring and the lake is about 2.7 km.

Figure 8 Map of lake Velencei and the location of the sampling site

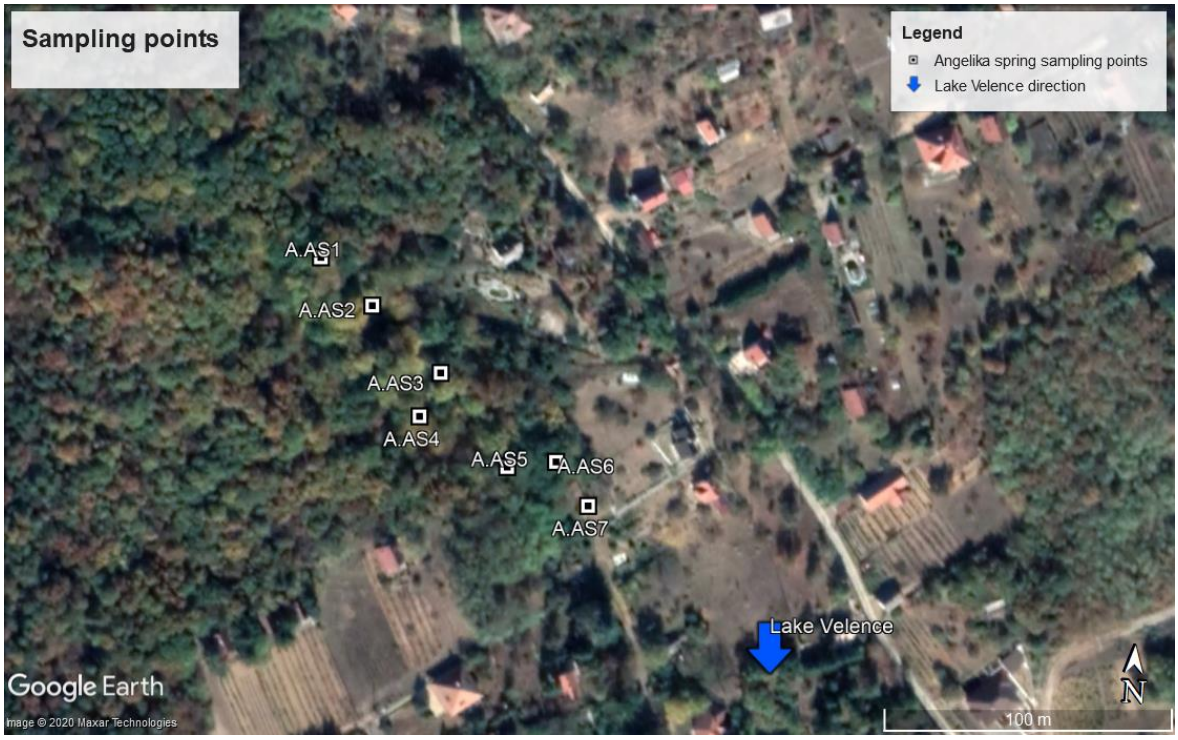

Figure 9 Arrangement of the sampling points - Eva Spring

The sample collection started at the point where the spring reaches the surface. It was possible to collect 7 samples from the spring at different places, although the spring vanished at certain places and then reappeared. The average depth of the creek at the sampling points was between 2 cm and 3 cm and the sites were muddy due to the shallowness of the water. Once the samples were taken at the beginning of the spring season, the ground was full of dry leaves and the volume of water was not high. The samples were cataloged as shown on the *Table 4* below. It is nice to write something the real precipitation values at that time, and some weeks before.

Table 4 Eva Spring sample information (April 12th, 2010)

Sample name	Coordinates	Sample Time
A.ES1	47°14’46.7” N 18°35’13.2” E	14:45
A.ES2	47°14’46.2” N 18°35’14.1” E	14:57
A.ES3	47°14’45.5” N 18°35’15.3” E	15:02
A.ES4	47°14’45.0” N 18°35’15.0” E	15:07
A.ES5	47°14’44.5” N 18°35’16.5” E	15:14
A.ES6	47°14’44.6” N 18°35’17.3” E	15:21
A.ES7	47°13’56.1” N 18°35’51.8” E	15:25

4. RESULTS AND DISCUSSION

All the values measured by Liquid Scintillation Analysis and those values derived from these ones are shown in Table 5. Analyzing the spectrum, it is possible to notice that there is a peak in the rage of 350 keVee and 450 keVee which correspond to the decaying energy of the radon atoms. The peak was compared with the background values to distinguish the results in two groups:

- Group I: Significant radon concentration
- Group II: Close to background radon concentration

Therefore, sample concentration could have a strong meaning, in this case it represents the existence of the radon concentration that could be found on the site.

The formulas and equations used to obtain the values of Decay Time, Decay Loss, Radon Concentration (measurement), Radon Concentration (sampling), Number of Decays (original and measured), Uncertainty of the Measurement Concentration and Activity are shown below.

The measurement of detected intensity is the number of counts per minute (CPM) of radon in the samples. Knowing that the background is 11.29 Bq/l (according to a parallel study mentioned before and considering that the OptiFlur O was used) and the calibration constant of the device is 1.96 it was found the concentration in the moment of the measurement (Cm) using the formula:

$$\boldsymbol{C_m = \frac{CPM - 11.29}{1.96}} \quad (\boldsymbol{Unit}: \boldsymbol{\frac{Bq}{l}}) \qquad \text{Eq.5}$$

It was also relevant to calculate the decay constant (λ) by applying the half-life of radon ($T_{1/2}$) which is equal to 3.86 days and then using the following equation:

$$\boldsymbol{\lambda = \frac{ln\,2}{T_{1/2}}} \qquad \text{Eq.6}$$

To calculate the decay loss of radon, we need the decay constant (λ) and the time difference between sampling time and measurement time (Δt) in days. Finally, were applied all these values in the following formula to find the decay loss of radon in this period:

$$\boldsymbol{Decay\ loss} = \boldsymbol{e^{-\lambda.\Delta t}} \qquad \text{Eq.7}$$

Using the values of decay loss and radon concentration in the time of measurement (Cm), it was calculated the concentration in the time of sampling (Cs) which is the radon concentration in the water at the moment of the sampling. To determine Cs, we used the following equation:

$$\boldsymbol{C_s} = \frac{\boldsymbol{C_m}}{\boldsymbol{e^{-\lambda.\Delta t}}} \qquad (\boldsymbol{Unit}: \frac{\boldsymbol{Bq}}{\boldsymbol{l}}) \qquad \text{Eq.8}$$

The number of decays in the time of the of the 10 ml sample (N_m) was determined using the values of counts per minute (CPM) found by Liquid Scintillation Spectroscopy and the total time spent to measure the samples that was of 15 minutes. So, we used the following equation to determine the number of decays:

$$\boldsymbol{N_m} = \boldsymbol{CPM} * \mathbf{15} \qquad \text{Eq.9}$$

Moreover, the total uncertainty of this measurement (σ_{Cm}) in percentage was calculated summing the percentage of the uncertainty given by the measuring device (σ_{CPM}) to the background (BG) uncertainty (σ_{BG}) that we assumed as 3% and the calibration constant (CC) uncertainty (σ_{CC}) which was assumed as 2%. Then, the total uncertainty of this measurement was calculated using the following equation:

$$\boldsymbol{\sigma_{Co}} = \sqrt{\boldsymbol{\sigma_{CPM}}^2 + \boldsymbol{\sigma_{BG}}^2 + \boldsymbol{\sigma_{Cm}}^2 + \boldsymbol{\sigma_{CC}}^2} * \frac{\tau}{CC} \qquad \text{Eq.10}$$

$$\tau = \boldsymbol{e^{\lambda.\Delta t}} \qquad \text{Eq.11}$$

Additionally, the activity (Bq) of the sample was calculated through the period from sampling until measurement. For that, we used the values of decay constant (λ) and number of radon atoms from radon content (N_m). So, we have the following expression:

$$\boldsymbol{A} = \boldsymbol{\lambda} * \boldsymbol{N_m} \qquad \text{Eq.12}$$

On the other hand, we can also determine the number of radon atoms that was originally in the water at the sampling time (N_S). For that, we use the number of decays in the time of measurement (Nm) and the decay loss (***Eq.7***). Then, we have the following equation:

$$N_S = \frac{N_m}{Decay\ loss} \qquad \text{Eq.13}$$

During the measurement using Liquid Scintillation Spectroscopy, we were able to calculate the radon concentration in the vial after a specific time after the sampling procedure. As discussed and shown in the analysis report, the number of radon has been decayed since the sampling procedure. And as already shown in the steps above, it was possible to determine the original radon concentration in the water using the exponential decay law (Δt denotes the time between the measurement and the sampling:

$$C_M = C_S * e^{-\lambda.\Delta t} \qquad \text{Eq.14}$$

All the data obtained by analytical techniques and those ones calculated from these measurements are shown in the next subchapters. These values provide the radon concentrations in the time of sampling and in the time of measurement, the radon loss through a specific period of time, number of decays, activity, uncertainties, among other values.

Table 5 Compilation of measurement results and calculation

Sample Name	CPM	Measurement Concentration (Bq/L)	Sample Concentration (Bq/L)	Uncertainty (%)	Activity (Bq)
T1A	13.33	1.03	1.07	97.6	19.15
T2A	11.93	0.32	0.35	291.4	17.14
T3A	12.20	0.46	0.50	207.6	17.53
T1A_3h	12.49	0.61	0.76	62.7	19.15
T2A_3h	12.83	0.78	1.24	50.0	17.14
A.ES1	221.07	105.95	110.30	5.7	317.58
A.ES2	14.47	1.61	1.68	65.8	20.79
A.ES3	16.40	2.58	2.72	44.1	23.56
A.ES4	13.67	1.20	1.49	84.9	19.64
A.ES5	155.20	72.68	90.12	6.5	222.96
A.ES6	41.33	15.17	19.07	13.2	59.37
A.ES7	23.27	6.05	7.67	23.2	33.43

4.1. Danube Samples

Samples taken at the Danube river were brought to the lab and analyzed using the TriCarb 1000 so the radon concentration and the activity could be known.

The liquid scintillator gave the measurement in the form of a spectrum in which the radon concentration can be calculated. The spectrum and the calculation showed that the values of Danube samples were close to the background measurement. Therefore, all the samples taken from the Danube river would be part of the group I (Background concentration)

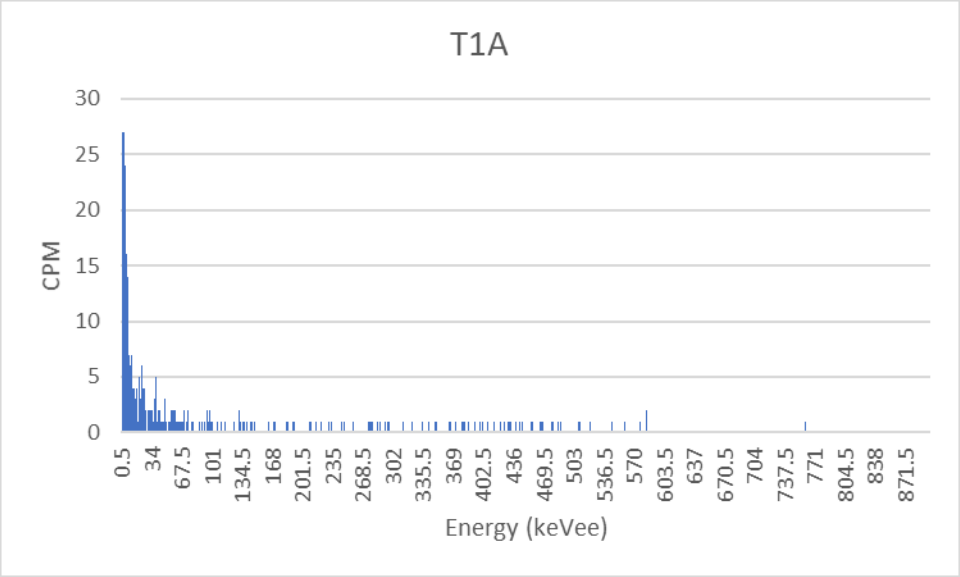

Figure 10 Spectrum of sample T1A (keVee)

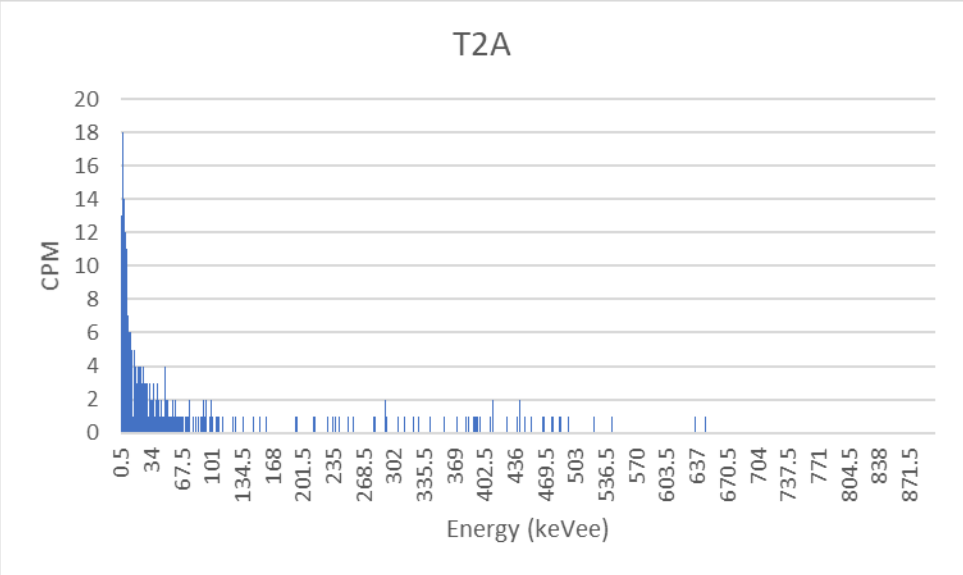

Figure 11 Spectrum of sample T2A (keVee)

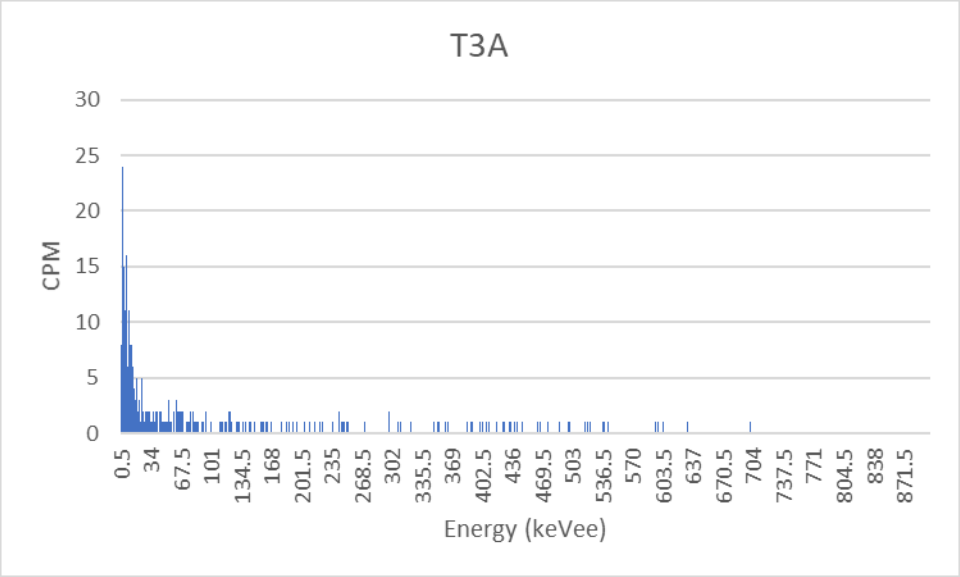

Figure 12 Spectrum of sample T3A (keVee)

The Danube river has a high discharge volume which can influence the radon concentration measurement even though there was a spring close to the sampling site.

4.2. Eva spring Samples

The results from the TriCarb showed a large variation in the radon concentration of the samples, as shown in the Table 5 and from Figure 13 to Figure 19.

The sampling points that had the higher radon concentration was the ones that had the spring water closer, indicating that the groundwater income was higher. The samples were taken in the transition between the winter and the spring, so the level of the stream was low, influenced mainly by the groundwater.

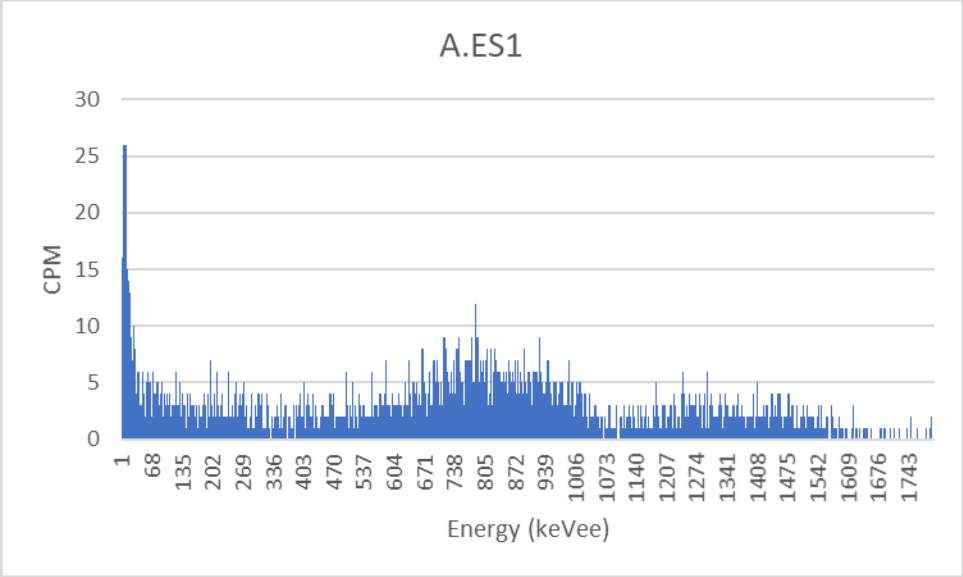

Figure 13 Spectrum of sample A.ES1 (keVee)

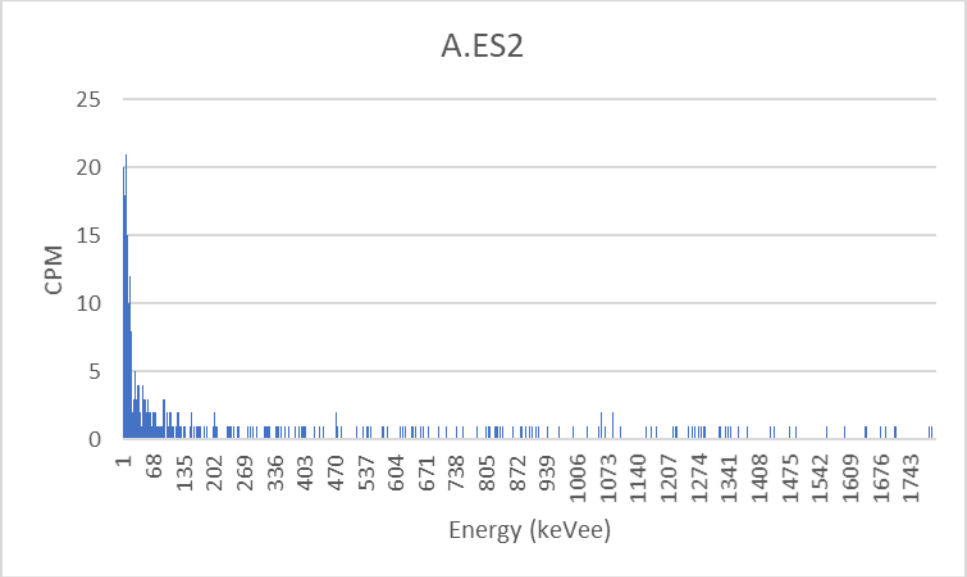

Figure 14 Spectrum of sample A.ES2 (keVee)

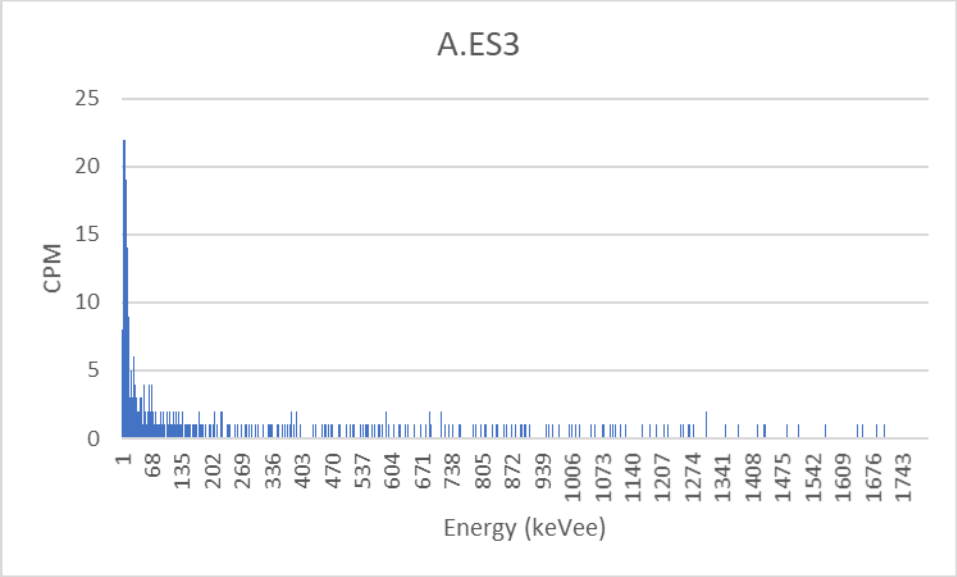

Figure 15 Spectrum of sample A.ES3 (keVee)

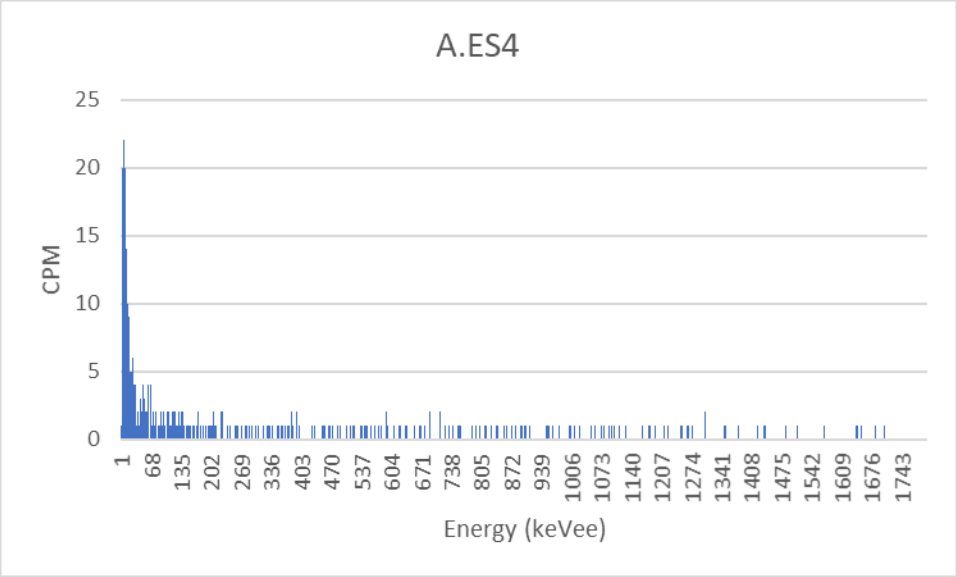

Figure 16 Spectrum of sample A.ES4 (keVee)

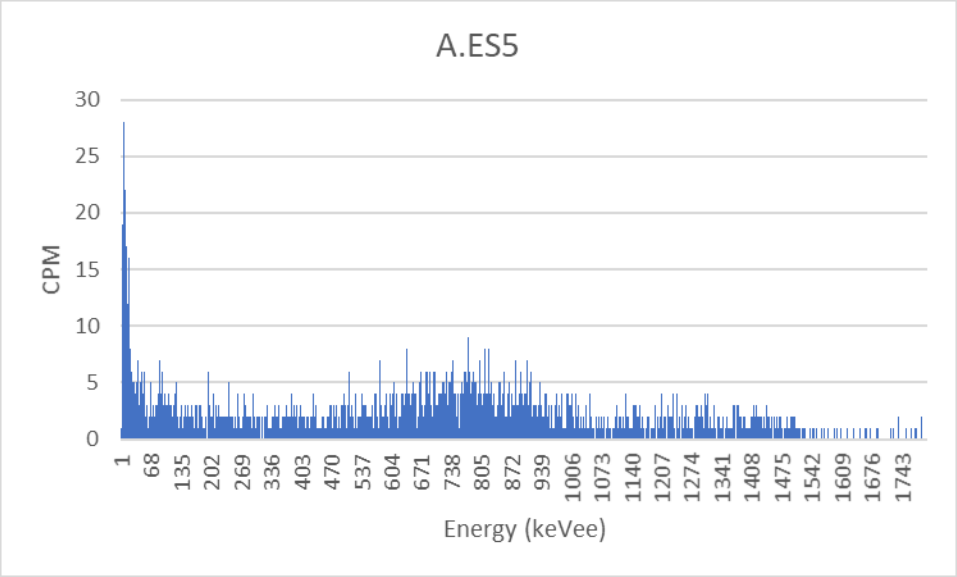

Figure 17 Spectrum of sample A.ES5 (keVee)

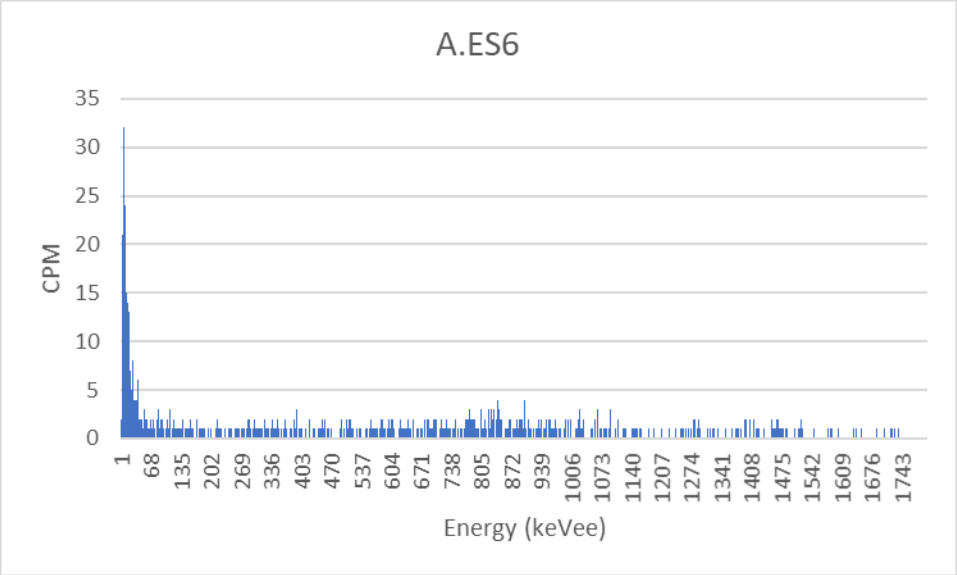

Figure 18 Spectrum of sample A.ES6 (keVee)

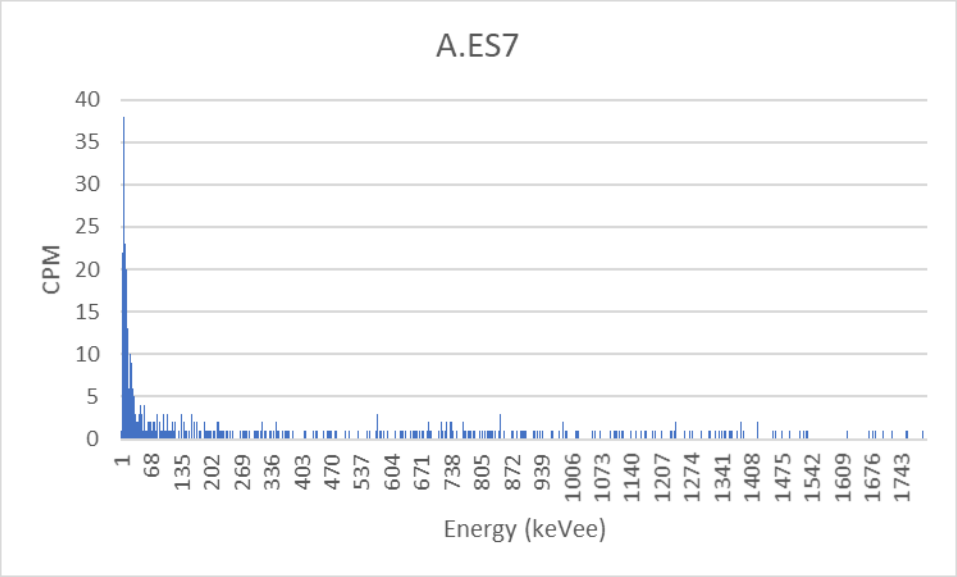

Figure 19 Spectrum of sample A.ES7 (keVee)

Analyzing the Eva spring samples, it was noticeable that the samples A.ES1 and A.ES5 fit into the group I and had anomalous radon concentration.

Since the weather conditions were stable with no considerable rain in the previous days, there were parts of the stream where it vanished and later on reappeared. It was very clear the where the stream once ran.

At the sampling point A.ES1, was the beginning of the stream, before there was no considerable volume of water to be sampled. The influence of the groundwater can be noticed once the radon concentration is much higher than the following sampling point. With around 4 meters apart, the sampling point A.ES2 has a decreased radon concentration which can indicate that the groundwater inflow is almost inexistent

5. CONCLUSIONS

After analyzing the methods, the TriCarb 1000 was chosen due to the availability of the instrumentation and practicality of using it. Liquid scintillation is a technique largely used with low uncertainty.

Since the radon is a noble gas, it easily diffuses and lower its concentration in the water what can explain the radon concentration of the samples in the group I.

The evidence of a high radon concentration is associated with a high-water volume income from the groundwater at that specific point of the sampling site. Radon is a natural tracer, and, during low levels of water, it was possible to acknowledge the places that the groundwater overflow to the surface.

Around the sampling point A.ES5, the second point where the radon concentration was the highest, there was a small dam where the water appears on the surface and accumulated. The water depth was around 3 cm, which may suggest a fresh income of groundwater at this spot. See Figure 20 below.

Figure 20 Sampling point A.ES5

The sampling points can be grouped as anomalous radon concentration and background concentration as summarized in the table 6. The measurement time of the Danube samples did not change the characteristic group of the samples.

Table 6 Sampling grouping

Sample Name	Characteristic group
T1A	I
T2A	I
T3A	I
A.ES1	II
A.ES2	I
A.ES3	I
A.ES4	I
A.ES5	II
A.ES6	I
A.ES7	I

It was possible to characterize the samples as significant radon concentration (I) and close to background radon concentration (II) due to its measurements. Only two samples could be described as significant radon concentration (A.ES1 and A.ES5) which could imply a discharge point at A.ES5. Both could be found in areas where most of the water income came from the groundwater.

BIBLIOGRAPHY

Chanyotha, S. et al., 2014. Prospecting for groundwater discharge in the canals of Bangkok via natural radon and thoron. *Journal of Hydrology,* 11, Volume 519, pp. 1485-1492.

Chapon, A., Pigrée, G., Putmans, V. & Rogel, G., 2016. Optimization of liquid scintillation measurements applied to smears and aqueous samples collected in industrial environments. *Results in Physics,* Volume 6, p. 50–58.

Csanád, M., Horváth, Á., Horváth, G. & Veres, G., 2012. *Environmental Physics Methods Laboratory Practices.* s.l.:s.n.

Curie, P., 1905. Radioactive substances, especially radium. *Radioactive Substances,* 6 6.

Dulaiova, H., Burnett, W. C., Wattayakorn, G. & Sojisuporn, P., 2006. Are groundwater inputs into river-dominated areas important? The Chao Phraya River - Gulf of Thailand. *Limnology and Oceanography,* 9, Volume 51, pp. 2232-2247.

Ferreira, V. V. M. et al., 2018. Use of radon isotopes, gamma radiation and dye tracers to study water interactions in a small stream in Brazil. *Environmental Earth Sciences,* 10.Volume 77.

Garcia-Solsona, E., Garcia-Orellana, J., Masqué, P. & Dulaiova, H., 2008. Uncertainties associated with 223Ra and 224Ra measurements in water via a Delayed Coincidence Counter (RaDeCC). *Marine Chemistry,* 4, Volume 109, pp. 198-219.

Geibert, W. et al., 2013. 226Ra determination via the rate of222Rn ingrowth with the Radium Delayed Coincidence Counter (RaDeCC). *Limnology and Oceanography: Methods,* 11, Volume 11, pp. 594-603.

Gyalog, L. & Horvath, I., 2004. *A Velencei-hegyseg es a Balatonfo foldtana/Geology of the Velence Hills and the Balatonfo.* s.l.:Magyar allami foldtani intezet Budapest.

Hatje, V. et al., 2017. Applications of radon and radium isotopes to determine submarine groundwater discharge and flushing times in Todos os Santos Bay, Brazil. *Journal of Environmental Radioactivity,* 11, Volume 178-179, pp. 136-146.

Lide, D. R., 1995. *CRC handbook of chemistry and physics: a ready-reference book of chemical and physical data.* s.l.:CRC press.

Mafra, K. C., 2011. *Medidas da Concentração de Radonio-222 em água de poço e solo da região do Pinheirinho em Curitiba e proposta de mitigação da água,* s.l.: s.n.

Rahman, S., Faheem, M. & others, 2008. Natural radioactivity measurements in Pakistan—an overview. *Journal of Radiological Protection,* Volume 28, p. 443.

Salih, N. F., Jafri, Z. M. & Aswood, M. S., 2016. Measurement of radon concentration in blood and urine samples collected from female cancer patients using RAD7. *Journal of Radiation Research and Applied Sciences,* Volume 9, p. 332–336.

Silva, L. A. et al., 2017. Solubilidade e reatividade de gases. *Química Nova,* 3.

Sophocleous, M., 2002. Interactions between groundwater and surface water: the state of the science. *Hydrogeology Journal,* 1, Volume 10, pp. 52-67.

STATEMENT

Name: Amanda Lafetá Oliveira
Neptun ID: JTSYGD

ELTE Faculty of Science: MSc Environmental Sciences

specialization: Physics

Title of diploma work: Investigation of the interaction between groundwater and surface water at discharge area in Hungary

As the author of the diploma work I declare, with disciplinary responsibility that my thesis is my own intellectual product and the result of my own work. Furthermore I declare that I have consistently applied the standard rules of references and citations.

I acknowledge that the following cases are considered plagiarism:
– using a literal quotation without quotation mark and adding citation;
– referencing content without citing the source;
– representing another person's published thoughts as my own thoughts.

Furthermore, I declare that the printed and electronical versions of the submitted diploma work are textually and contextually identical.

Budapest. June 2, 2020

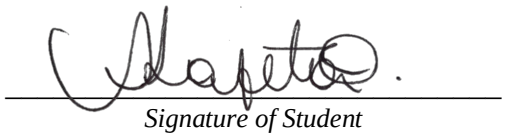

Signature of Student